LATTICE BEAM DYNAMICS STUDY AT LOW B FOR SARAF/EURISOL DRIVER 40/60 MEV 4 MA D&P SUPERCONDUCTING LINAC

J. Rodnizki, B. Bazak, D. Berkovits, G. Feinberg, S. Halfon, A. Pernick, A. Shor,
Y. Yanay, Soreq, Yavne 81800, Israel

Abstract

In this study we examine a lattice for the SARAF superconducting (SC) linac at the low-β range. The SC Half Wave Resonator cavities in the first cryostat are optimized for a geometric β_0=0.09 and hence the β=0.0567 ions coming from the RFQ are mismatched. We developed a semi adiabatic tuning method for the low-β portion of the SC linac. The guidelines were derived from the study of two linac lattices that were considered for the SARAF 40 MeV proton and deuteron linac, extended up to 60 MeV for the low energy part of the EURISOL driver. Simulations were run using the TRACK and GPT codes. The lattices were tested for energy gain along the linac, emittance growth and acceptance. Further, error runs in GPT using a tail emphasis technique to enhance statistics by focusing on the bunch tail allowed us to examine compatibility of the lattices with hands-on maintenance requirements. Our study may be relevant for other linacs that begin with SC cavities immediately following the RFQ, such as SPIRAL2, and perhaps also for IFMIF which is designed to start with similar β–mismatch at the low-β range.

INTRODUCTION

In this study we examine a lattice for the SARAF [1] superconducting (SC) linac at the low velocity (β) range. The accelerator at SARAF is composed of an ion-source, a 4-rod 176 MHz 1.5 MeV/u RFQ and a 40 MeV proton and deuteron SC linac. The SC accelerator is described in details in [2] and the accelerator front-end in [3,4,5]. Motivated by the lower construction and operation costs, the SARAF linac starts with SC independent phase 2-gap HWR cavities, right after the RFQ. The common solution of DTL in this transition (between the RFQ and the SC linac) was rejected in order to have an efficient high energy gain acceleration of a large range of mass over charge ratio (*M/q*=1…2) ions. The SC Half Wave Resonator (HWR) cavities at the first cryostat are optimized for a geometric β_0=0.09 and hence the β=0.0567 ions from the RFQ are mismatched. The development of an additional SC cavity with β_0 at the range of 0.06 at 176 MHz seemed to be technically complicated due to inner surface treatment in such a narrow gaps size. The effort to accelerate light ions at the low-β range with SC linac in a high acceleration rate is limited by the induced strong longitudinal focusing force [6]. High accelerating gradient could introduce high longitudinal phase advance resulting in beam losses [7]. A tuning method was developed for the low-β side of the accelerator, which faces the dual problem of mismatched velocity and over focusing at high acceleration gradient. A preliminary approach of this method is applied to the SARAF 40 MeV deuteron accelerator. We developed a new approach for beam loss calculations that places emphasis on the tails of the particle distributions. This scheme is used for simulating the SARAF accelerator at a sensitivity of the hands-on maintenance criterion. The simulations are presented at the end of this paper, including error analysis, and are able to predict a reliable beam loss value, using a single PC.

BEAM TUNING METHOD

For multi gap cavities, the problematic region for the tune is the low β section. In this area the acceleration in each gap is quite large in comparison to the particles initial velocity at the cavity entrance. The particle deviation from the reference particle at the second gap of the cavity depends on the velocity gain of the particle at the first gap. The evaluation of the particle's trajectory, with significant velocity increase along the cavity, has to be performed at each gap separately, taking into account the particles phase deviation from the reference particle at each gap [8, p.189]. If the accelerating RF field along the bunch in one of the gaps deviates from the linear range it could introduce significant emittance growth during the acceleration. The range of the accelerated particle's phase- ϕ_i, at each gap i is defined by the reference particle phase ϕ_{ri} and the bunch half length- Ψ_i, $\phi_{ri} - \Psi_i \le \phi_i \le \phi_{ri} + \Psi_i$. Ψ_i is estimated from the phase distribution of the tuned bunch at the gap entrance.

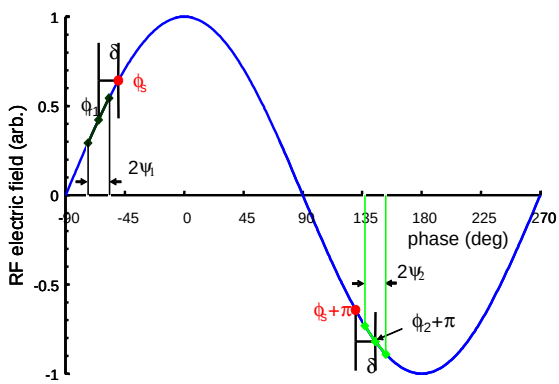

Figure 1: RF field as function of phase and phase definition for acceleration at β mismatch as defined in the text.

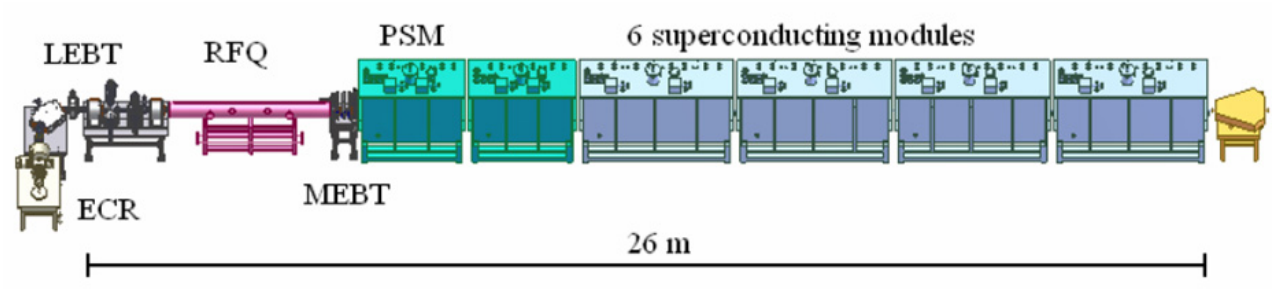

Figure 2: Schematic layout of the SARAF.

For a two gap cavity, i=1,2 (Fig. 1) the reference particle phase at each gap is evaluated from the synchronous phase ϕ_s:

$$\phi_{r1} = \phi_s - \delta \quad \phi_{r2} = \phi_s + \delta \quad \delta = (\beta_0 / \beta - 1) * \pi / 2$$

where δ is the difference between the synchronous phase and the reference particle phase at both gaps, β_0 is the geometric β of the cavity and β is the reference particle relative velocity at the first gap exit.

To minimize the emittance growth along the linac at the low β section, in each gap of the multi gap cavities, it is validated that the acceleration RF field is linear along the bunch. A key factor for a good tuning is of course a small bunch width along the linac. The longitudinal phase advance per unit length is kept constant (based on [8 p.175]). (The method developed here assumed a single cavity per period, further development is needed for few cavities in a period):

$$\frac{d(W - W_s)}{ds} = qV_0T(\cos\Phi - \cos\phi_s)/L$$

$$\frac{d(\Phi - \phi_s)}{ds} = (W - W_s)2\pi/(mc^2\gamma_s^3\beta_s^3\lambda)$$

$$k_{lo}^2 = -2\pi/(mc^2\gamma_s^3\beta_s^3\lambda)qV_0T\sin\phi_s / L$$

$$V_{02}T_2 = V_{01}T_1(\sin\phi_{s1}/\sin\phi_{s2})(\gamma_{s2}^3\beta_{s2}^3L_2)/$$

$$(\gamma_{s1}^3\beta_{s1}^3L_1)$$

where: W is the bunch particle energy, W_s is the synchronous particle energy, Φ is the approximated particle phase along the cavity gaps, q is the particle charge, L is the distance between cavities, k_{lo} is the phase advance per unit distance, V_0T is the energy gain at zero synchronous phase per unit charge at a cavity based on the cavity voltage V_0 (proportional to the cavity field amplitude) and the bunch transient time factor T, i is the cavity index (i=1 is the upstream cavity, i=2 is the cavity to tune) and s is the distance at the beam direction.

This formula implies that after applying a linear RF acceleration field along the bunch, in each gap, then, the energy gain of the cavity at zero synchronous phase ($V_{02}T_2$) is tuned according to the phase advance per unit length at the upstream cavity k_{lo}, in order to avoid significant local variations of the phase advance per unit length. The applied detuned phase advance per period σ_l is evaluated by: $\sigma_l = \int_0^L \frac{1}{\hat{\beta}(s)} ds$ where $\hat{\beta}$ is the Courant Snyder parameter [9 p. 15].

At the high β range, in order to maintain the acceleration efficiency, the synchronous phase is kept between -20 and -15 degrees, but not above -15 degrees in order to maintain stability. The transverse phase advance should be kept higher than 50% of the longitudinal phase advance to eliminate emittance growth and halo development [10].

LINAC LATTICE SETUP

The linac lattice is described in details in ref. [1-3] and references there in. The linac is matched transversely to the RFQ with three quads along the MEBT to convert the beam to a radial symmetric shape (Fig. 2). The linac is composed of two β_0=0.09 cryostats followed by four β_0=0.15 cryostats.

In this work two options for the SC linac are studied. The two are called here symmetric and asymmetric and are differing in the internal cryostat arrangement. Each period at the basic linac asymmetric configuration is composed of a leading SC solenoid followed by two SC cavities (Fig. 3). The first SC cavity of the linac is used as a buncher.

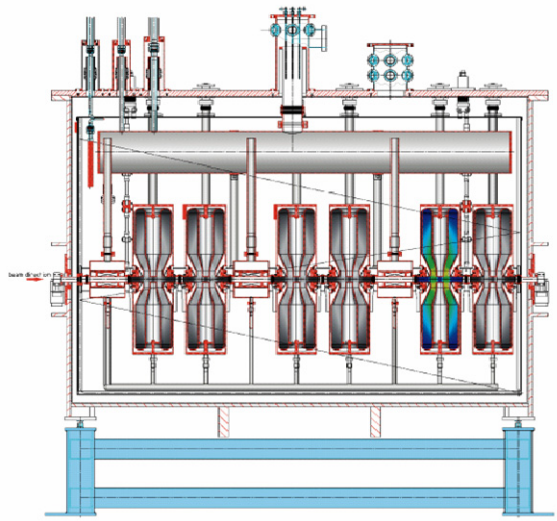

Figure 3: The Prototype Superconductor Module with the asymmetric lattice design [2].

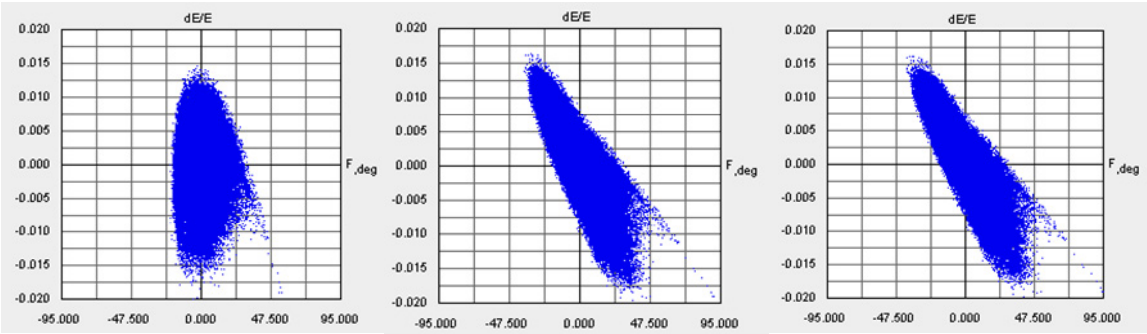

At the RFQ exit Symmetric first gap Asymmetric first gap

Figure 4: Longitudinal phase space at the RFQ exit and at the entrance to the SC linac.

At the symmetric lattice the distance between the first and the second MEBT quads is enlarged by 9 cm to increase the transverse focusing. In this case the linac starts with a leading cavity operated as a buncher so the RFQ to buncher distance is reduced by 16 cm with respect to the 107 cm distance in the asymmetric lattice. The first HWR at the asymmetric lattice start 30 cm downstream the warm to cold transition. This distance (partially inside the solenoid) acts as a cold trap in the first cryostat, which protects the SC cavities from contamination emerging from the injector. Both lattices enable acceleration of a 4 mA deuteron and proton CW beams up to 40 MeV. The lattice is extended by 3 more β_0=0.15 cryostats to reach 60 MeV as a preliminary option for the EURISOL driver. The current design of the EURISOL driver includes modifications such as using one HWR at each internal period of the β_0=0.09 cryostats downstream the RFQ [11].

"End to end" simulations of the SARAF linac have been performed using TRACK [12] from the 20 keV/u ion source to 40 MeV, extended to 60 MeV for the EURISOL driver and in GPT [13] from the RFQ entrance and up to 40 MeV. The 3D fields of the LEBT solenoids and the fringe fields of the LEBT bending magnet were modelled,. The RFQ accelerating structure was generated according to the RFQ design data [5], 3D fields were modelled for the radial matcher with EM Studio. The fields in the regular cells are presented by the 8-term Fourier Bessel expansion. The 3D fields of the SC solenoids were calculated and the 3D fields of the SC cavities were included in the simulation.

BEAM TUNING RESULTS AND COMPARISON

The longitudinal phase space diagram of 500k macro particles at the RFQ exit and at the entrance to the first HWR gap of the symmetric and the asymmetric lattice are

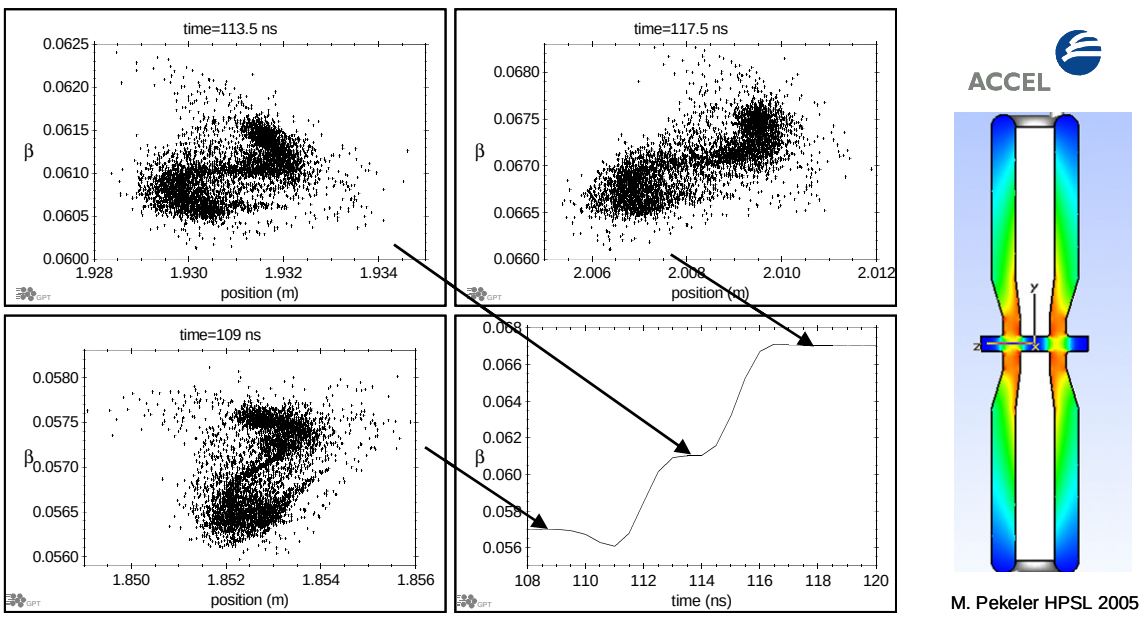

Figure 5: Longitudinal phase space along the first accelerating two gaps HWR after the buncher, 3.5 mA p beam.

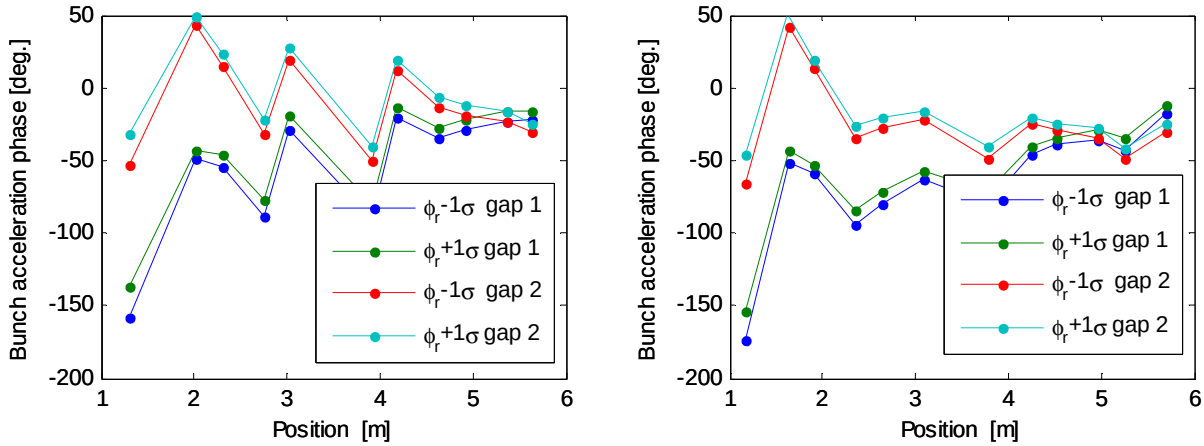

Figure 6: Asymmetric (left) and symmetric (right) lattice bunch acceleration phase at the first cavity gap (bottom curves) and the second gap (top curves) along the low β SC linac section.

presented in Fig. 4. The high longitudinal phase advance of the macro particles and the significant increase in β along the first accelerating cavity are presented in Fig. 5. These results are typical to accelerating light ions with a high accelerating field at low-β with a high β-mismatch. The RF phase is chosen so that the bunch encounters the RF field in its linear portion at each low-β gap using the accelerating phases shown in Fig. 6. The effort to bunch the beam along the linac is presented in Fig. 7. The deuteron energy at the linac exit for SARAF and for EURISOL is [42.2, 65.2] and [42.6, 66.0] MeV for the symmetric and the asymmetric lattices for a 4 mA deuteron beam (Fig. 8). The energy difference between the lattices is not significant. One can probably improve the asymmetric lattice by reducing the energy gain at the low β section. The emittance growth is similar at both lattices for the rms and 99.5% envelopes both for longitudinal and normalized transverse emittances. The maximum envelope of 500k macro particles is larger at the longitudinal phase space for the symmetric lattice and vice versa for the transverse phase space (Figs. 9 and 10). The symmetric lattice gives significantly higher acceptance than the asymmetric lattice (Fig. 11). The asymmetric acceptance can be improved by changing the buncher synchronous phase.

BEAM LOSS CRITERION

The beam loss criterion value was deduced from a limit on residual activation in the components bore radius along the linac. This was determined in order to limit the dose rate to 2 mrem/h (100 h of hands-on maintenance per technician per year gives 10% of the annual dose limit), at 30 cm away from beam line, 4 hours after accelerator shutdown after a full year of operation. The SARAF linac bore radius is built of about half stainless still and half niobium. The beam operation program is composed of about half deuterons beam time and half protons beam time. Earlier calculation showed that up to 40 MeV, the main contribution to the dose is due to deuterons (relative to protons) bombarding thick ^{56}Fe target (relative to niobium). Figure 12 presents the produced dose rate from 1 year of operation (by the relevant produced radioisotopes) along the 22 m linac followed by high energy beam line towards the targets. The results are normalized to 1 nA/m deuterons beam loss, with energy evolution as presented in Fig. 8. Figure 13 presents the decay of the dose from 4 hours until 1000 days after shutdown. Taking into account the linac composition and beam operation, relative to the above conservative calculation, a beam loss criterion of l nA/m was used for the linac design study.

ERROR RUNS AND BEAM LOSS USING THE TAIL EMPHASIS METHOD

We have applied the tail emphasis method [14] in order to study particle losses along the linac for the asymmetric lattice (Fig. 14). The method is based on the assumption that losses begin longitudinally, and problem particle begin at the periphery of the longitudinal phase space at the RFQ exit, and originate in the boundaries between the downstream bunches at the dc current entering the RFQ buncher section. The method allows us to calculate losses along the linac at the 1 nA level with limited computational efforts: A Tail Emphasis deuteron beam with 2.1 million macro particles at the RFQ entrance is equivalent to the simulation of 3 bunches containing 42.6 million macro-particles (each 1:10, equivalent to 0.3 nA) for 4mA CW at 176 MHz.

The reduced computation time allows us to run a large number of simulations in a relatively short span of time. This allows us to explore the effect of manufacture and operational errors on the beam and estimate losses due to these factors, as described in [15]. Table 1 summarizes the range of the static and dynamic errors used in the study. Static errors are assumed to have a uniform distribution distributed within the limits shown on the table. Dynamic errors are assumed to have a Gaussian distribution with a standard deviation as specified in the table. A series of error runs were performed for an input deuteron beam at the RFQ exit. This input is generated by simulating the

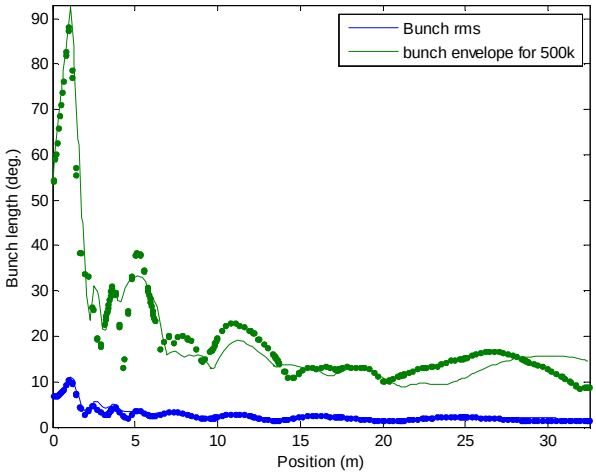

Figure 7: Bunch amplitude length for the symmetric (dots) and the asymmetric (solid line) lattices.

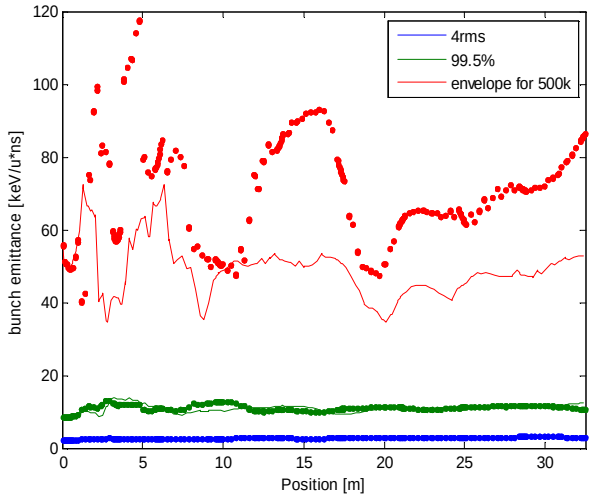

Figure 9: Bunch longitudinal emittance for the symmetric (dots) and the asymmetric (solid line) lattices

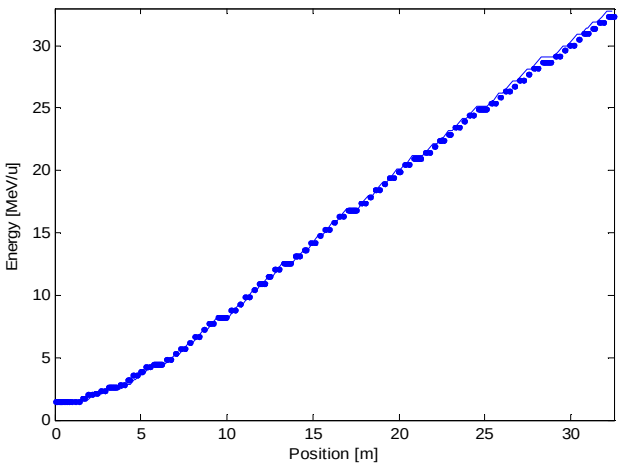

Figure 8: Bunch energy along the linac for the symmetric (dots) and the asymmetric (solid line) lattices.

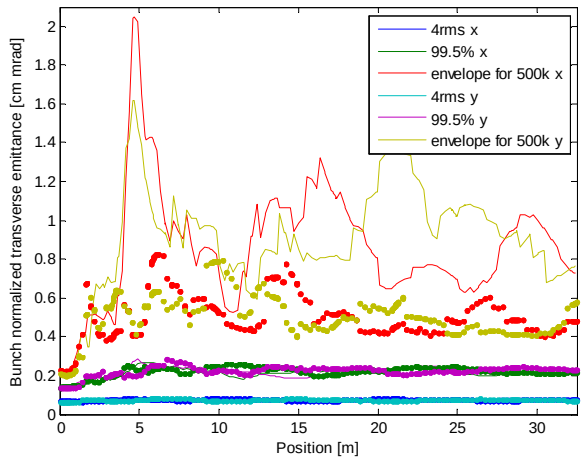

Figure 10: Bunch transverse normalized emittance for the symmetric (dots) and the asymmetric (solid line) lattices.

RFQ with an entrance normalized transverse rms emittance of 0.2 π mm mrad. The tail emphasis method was applied within the GPT [13] code to run the beam dynamics simulations A similar error set was then generated with a doubled dynamic phase error to study the sensitivity of the realizations to larger phase errors at the HWR accelerating fields. For the input 0.2 π mm mrad both error runs were without losses, as shown in Fig. 15. However, according to the on site tests and the specifications the transverse normalized rms emittance at the RFQ exit is 0.3 π mm mrad. The simulated transverse macro particle phase space at the RFQ exit was expanded to reach this value (Fig. 16), and the error runs were repeated for the new bunch, having the specified 0.3 π mm mrad rms normalized emittance at the RFQ exit. These error runs were conducted with the nominal phase error. Figure 17 shows the results. For two out of the 50 linac realizations (Fig. 17a,b) the lost particles exceeded the design beam lost criterion (1 nA/m).

Table 1: Fabrication misalignment and operation errors

Component	Error	Static	Dynamic
Quadruple	Misalignment x,y,z [mm]	±0.2	
	Rotation θ [mrad]	±3	
	Magnetic field [%]	±2	0.5
Solenoid	Misalignment x,y,z [mm]	±0.2	
	Magnetic field [%]	±2	0.5
HWR	Misalignment x,y,z [mm]	±0.4	
	Rotation θ [mrad]	±6	
	field amplitude[%]	±2	0.5
	Phase [degree]	±1	0.25

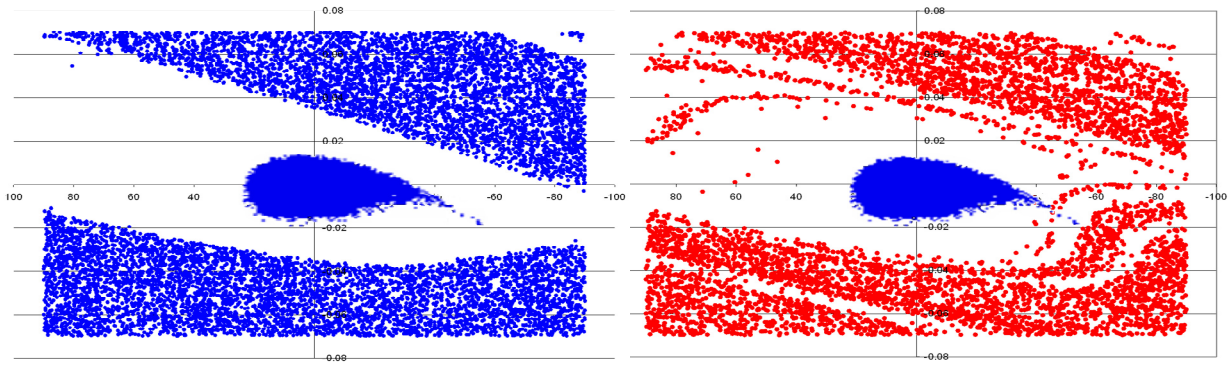

Figure 11: Longitudinal phase space acceptance for the symmetric (left) and the asymmetric (right) lattices vs. the bunch spread at the RFQ exit (relative energy spread vs. phase (deg)).

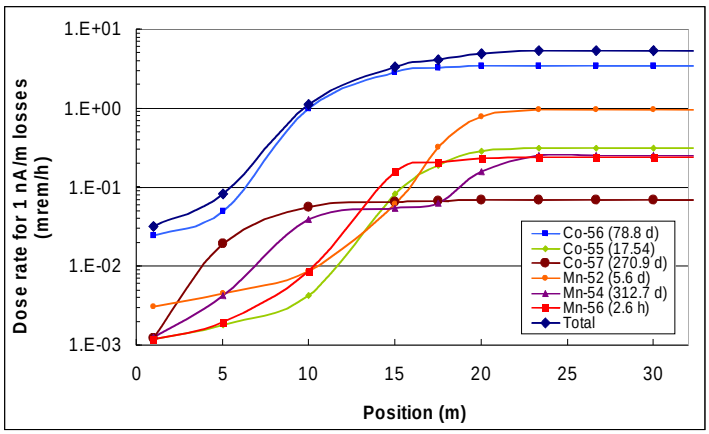

Figure 12: Dose rate residual activity calculated for uniform 1 nA/m deuteron beam loss on ^{56}Fe target along the SC linac and the HEBT, after one full year of operation, 4 hour after shut down and at a distance of 30 cm from the beam line.

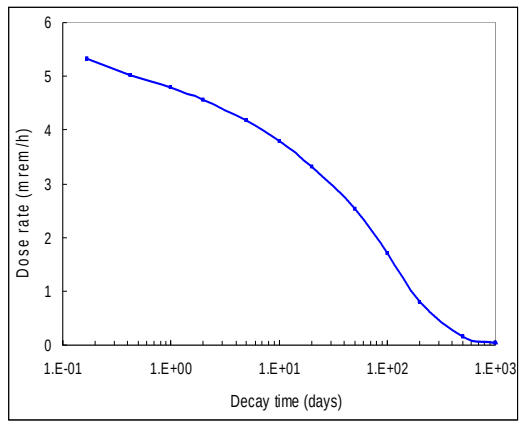

Figure 13: Residual activity dose rate (of Fig. 12) decay after shut down.

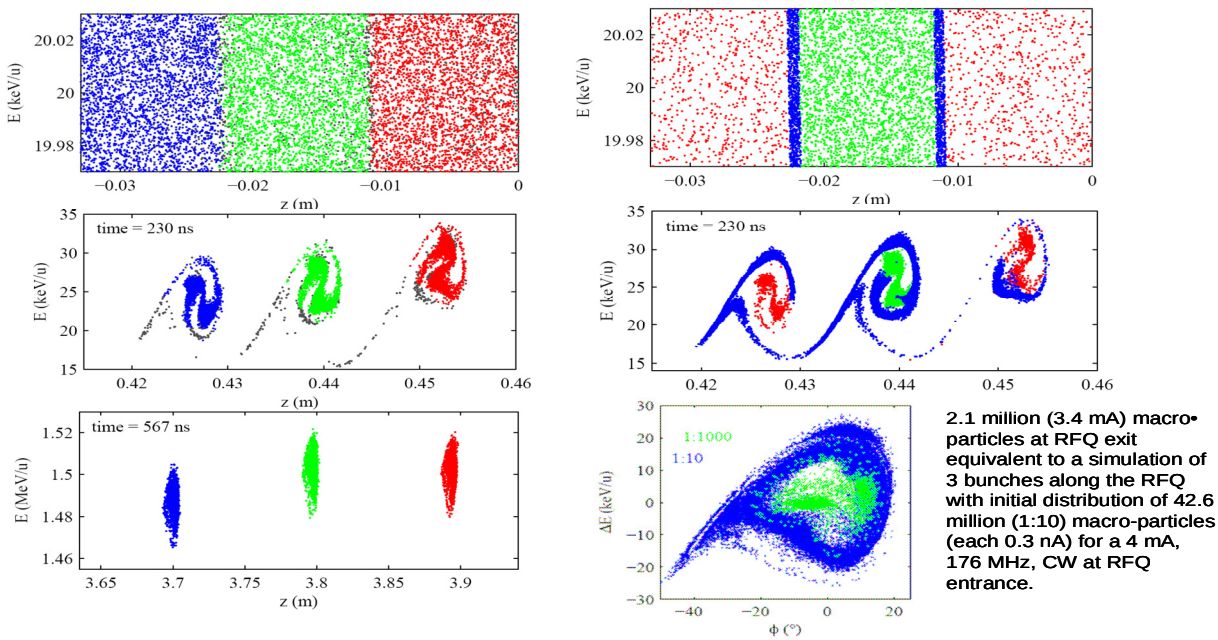

Figure 14: Longitudinal phase space along the RFQ. Top – entrance. Middle – end of bunching section. Bottom – exit. Three bunches are presented. The tail emphasis method (right) enable us increase the resolution in the longitudinal phase space tail (1 macro particle per 10) and to reduce the resolution in the neighbour bunches relative to the regular treatment (left).

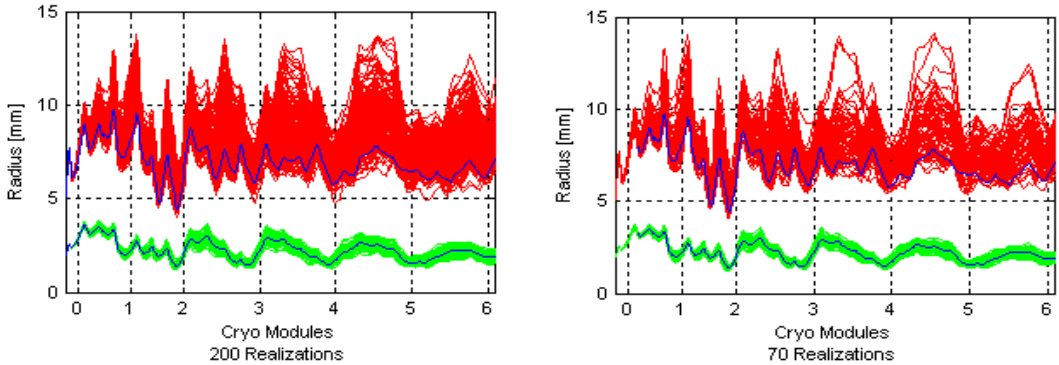

Figure 15: Transverse envelope and rms radius for series of error runs. Left: standard run. Right: dynamic phase errors doubled. Showing results for 32k/193k core/tail particle distribution with a normalized rms input emittance of 0.2 mm mrad, 3.4 mA d beam, at RFQ exit. The last macro particle is equivalent to 1 nA current. The bore radius is 19 mm within solenoids and 15 mm everywhere else.

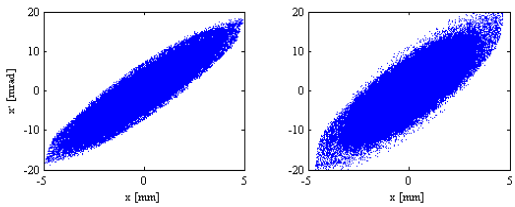

Figure 16: Simulated transverse phase space (left: original) is expanded to 0.3 mm mrad (right) to match the measured rms emittance at the RFQ exit

At one of the two runs the 31 lost macro particles (1 nA each) were lost at energy of 5 MeV. Practically, the evaluated exposure rate based on this realization is lower than 2mrem/h (required for hands on maintenance). Each realization represents a momentary configuration of the fields dynamic errors combined with static lattice errors. If the major source of losses is the dynamic errors we might consider the average beam loss, as shown in Fig. 17c, and that remains within the required hands on limits. We are currently conducting further simulations to verify it.

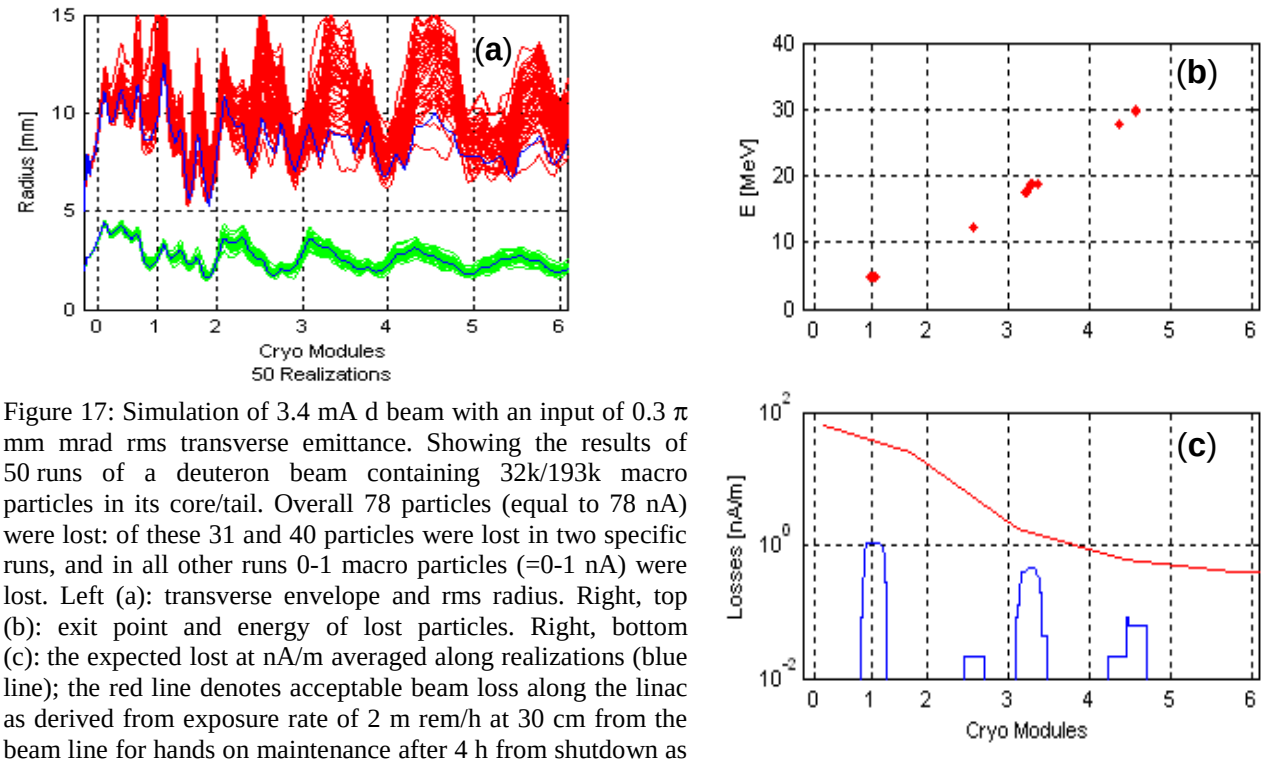

Figure 17: Simulation of 3.4 mA d beam with an input of 0.3 π mm mrad rms transverse emittance. Showing the results of 50 runs of a deuteron beam containing 32k/193k macro particles in its core/tail. Overall 78 particles (equal to 78 nA) were lost: of these 31 and 40 particles were lost in two specific runs, and in all other runs 0-1 macro particles (=0-1 nA) were lost. Left (a): transverse envelope and rms radius. Right, top (b): exit point and energy of lost particles. Right, bottom (c): the expected lost at nA/m averaged along realizations (blue line); the red line denotes acceptable beam loss along the linac as derived from exposure rate of 2 m rem/h at 30 cm from the beam line for hands on maintenance after 4 h from shutdown as explained in the section above (Fig. 12).

SUMMARY

A lattice consist of a SC linac at the RFQ exit designed for light ions that have variable mass to charge ratio probably will need a dedicated tune method to allow acceleration at low β with a β mismatch. A method to accelerate efficiently at the low β range was derived and applied for two basic lattices symmetric and asymmetric lattice. The symmetric lattice seemed to be the favour lattice since it has a better acceptance and since its transverse envelope seemed to be easier to control. A beam loss criterion for hands on maintenance was derived, 2 mrem/h at 30 cm from the beam line, and related to the expected simulated beam lost, nA/m, along the linac. The tail emphasis method enables us to increase the resolution to evaluate the lost particles at nA/m out of 4 mA nominal current for the required beam loss criterion for series of error runs. The method assumes that the lost particles are getting radical values at the RFQ bunching section at the longitudinal phase space. The expected exposure for the asymmetric lattice, the current lattice of the PSM stands at the bean loss criterion of hands on maintenance assuming the series of errors run are dominated by the dynamics errors.

REFERENCES

[1] A. Nagler, I. Mardor, D. Berkovits, K. Dunkel, M. Pekeler, C. Piel, P. vom Stein and H. Vogel, proceedings of LINAC 2006, Knoxville, Tennessee, MOP054 (2006) 168-170.

[2] M. Pekeler, K. Dunkel, C. Piel and P. vom Stein, "Development of a superconducting rf module for acceleration of protons and deuterons at very low energy", Proceedings of LINAC 2006, Knoxville, Tennessee USA TUP034 (2006) 321-323.

[3] C. Piel, K. Dunkel, M. Pekeler, H. Vogel, P. vom Stein, "Beam operation of the SARAF light ion injector", Proceedings of PAC07, Albuquerque, New Mexico, USA, TUPAN011 (2007) 1410-1412.

[4] C. Piel, K. Dunkel, F. Kremer, M. Pekeler, P. vom Stein, D. Berkovits, I. Mardor, "Phase 1 Commissioning Status of the 40 MeV Proton/Deuteron Accelerator SARAF" EPAC08, Genova, June (2008) 3452-3454.

[5] J. Rodnizki, B. Bazak, D. Berkovits, G. Feinberg, A. Shor, Y. Yanay, K. Dunkel, C. Piel, "Beam Dynamics Simulation of the 1.5 MeV Proton Beam Measured at the SARAF RFQ Exit", EPAC08, Genova, June (2008) 3458-3460.

[6] Thomas P. Wangler "Longitudinal Beam Dynamics Constraint on Accelerating Gradient in a Proton Superconducting Linac", American Physical Society meeting, Albuquerque New Mexico, 20-23 April (2002), http://www.eps.org/aps/meet/APR02/baps/abs/S2660001.html

[7] R. W. Granett, T. P. Wangler, F. L. Krawczyk and J. P. Kelley, "Conceptual design of a low-β SC proton LINAC", Proc. of PAC2001, Chicago, June 18-22, (2001) 3293.

[8] T. P. Wangler, Principles of RF Linear Accelerators, John Wiley and Sons, Inc., 1998.

[9] M. Reiser, Theory and Design of Charged Particle Beams, J. Wiley & Sons, Inc., 1994.

[10] P. N. Ostroumov, DESIGN FEATURES OF HIGH-INTENSITY MEDIUM-ENERGY SC HEAVY-ION LINAC, proceedings of LINAC 2002, Gyeongju, Korea, MO412 (2002) 64-66.

[11] A. Facco, A. Balabin, R. Paparella, D. Zenere, D. Berkovits, J. Rodnizki, J. L. Biarrotte, S. Bousson, A. Ponton, R. Duperrier, D. Uriot, V. Zvyagintsev, Beam Dynamics Studies on the EURISOL Driver Accelerator, Proceedings of the 2006 Linear Accelerator Conference, Victoria, British Columbia, Canada, 2008

[12] P. N. Ostroumov, V. Aseev and B. Mustapha, "TRACK a code for beam dynamics simulations in accelerators and transport lines with 3D electric and magnetic fields", ANL, March 27, 2006.

[13] General Particle Tracer (GPT), Pulsar Physics, http://www.plusar.nl/gpt/

[14] B. Bazak A. Shor, D. Berkovits, G. Feinberg, J. Rodnizki and Y. Yanay, Simulations of ion beam loss in RF linacs with emphasis on tails of particle distributions, to be published.

[15] J. Rodnizki, D. Berkovits, K. Lavie, I. Mardor, A. Shor, Y. Yanay, K. Dunkel, C. Piel, A. Facco and V. Zviagintsev, Beam Dynamics Simulation of the SARAF Accelerator Including Error Propagation and Implications for the EURISOL Driver, Proceedings of the 2006 Linear Accelerator Conference, Knoxville, 2006, p. 426.